Aerodynamic Performance of the HMS Sirius

Jonathon McCowan

Abstract

The Sinking of the HMS Sirius is known as one of Australia's most devastating maritime disasters which essentially put the entire future of the nation at risk. To better explain this event, research into the details and even the sailing characteristics of the HMS Sirius are being undertaken to better explain the event itself. One such characteristic is the aerodynamic performance of the vessel itself. To investigate this a scale model of the HMS Sirius, focusing on the sail plan was created by using draft images and estimations via examining vessels of the same era and or design, specifically the HMS Endeavour. The model was tested in a wind tunnel to determine forces generated in different sail conditions including the angle of the yards in relation to the hull. Using further research into hull resistance and manoeuvring characteristic e.g., leeway angle, a determination of whether the incident could have been avoidable can be established.

Keywords

Wind tunnel, drive force, side force, yard, mast, leeway angle, wind velocity, make way.

Nomenclature

Notation	Description	Nominal Unit
V	Wind Velocity	m/s
ρ	Density of the fluid (air density)	Kg/m^3
Re	Reynolds number	N/A
° Sail	Degree sail represents the angle of the yards in relation to the vessel centerline (0°, 30° and 60° Sail)	°
D-Force	Drive force is the force that propels the vessel forward and is aligned with the vertical center line of the model	newtons (N)
S-Force	Side force is the force that pushes on the side of the vessel and acts perpendicular to the model.	newtons (N)
C_{DF}	The drive force coefficient	N/A
C_{SF}	The side force coefficient	N/A
Leeway Angle	The angle difference between the heading and the actual direction of motion of the vessel.	°
VPP	Velocity predicted program	N/A

1 Introduction

The HMS Sirius was wrecked off the coast of Norfolk Island on the 19th of March 1790. As the Sirius was unloading supplies to the fledgling colony, she began to drift towards shore. To avoid the reef of Slaughter Bay the Sirius set sail to return to sea, however a change in wind direction prevented the vessel from weathering the western end of the bay.

Unable to tack, the Sirius was trapped in the bay and the prevailing winds and currents forced the vessel on the reef. With the vessel run aground, the hull suffered damage and it remained on the reef being destroyed over the coming weeks (Naval Historical society of Australia , 1994).

The sinking of the HMS Sirius being renowned in Australian maritime history for its impact to the fledgling colony, however due to the ship never being reconstructed, it is unknown how she would have handled the conditions and therefore it is unclear if the vessel could have been saved. For this reason, research is being done to find relevant hydrodynamic and aerodynamic characteristics of the ship. This research project poses the question, *"what are the aerodynamic characteristics of the HMS Sirius with only square sails and under what conditions could the vessel have generated enough aerodynamic drive force in order to make way"?*

To answer this question, a scale model representing the sail plan needed to be created which will then be tested in a wind tunnel to find the aerodynamic efficiency of the sail plan.

1.1 Literature Review

Traditionally, sailing vessels were the main form of propulsion for maritime transport however with the invention and advancement of motorized propulsion, sailing has become more of a sport or hobby. Even if sailing vessels are no longer the norm, there are still many traditionally rigged sailing vessels around today (MI News Network, 2021). Because square rigged ships can have a multitude of sail configurations there exists some research into the aerodynamics of these vessels, especially focusing on the survivability in severe weather and testing different combinations of sails. Due to this the experimentation, and papers relating to this project specifically are hard to find, and most papers are related to a vessel that is still existing today, making the model development and full-scale validation easier.

In 2002, Barry Deakin produced a paper on sailing ship performance. Using the vessel *S.V. Tenacious*, a series of comprehensive model tests were undertaken during the design and construction of the square-rigged vessel (Figure 1). These results were then correlated with the full-scale ship after construction. For wind tunnel testing a 1:30 scale model was created with full sail and rigging and pivoting yard arms were also added. The wind tunnel used has a working section of 3.7m height and 4.6m width and six component balance to provide a complete matrix of forces and moments (Deakin, 2002).

Figure 1 Scale model of the S.V. Tenacious inside the university of Southampton wind tunnel

The objective of the wind tunnel testing ranged from finding data for a VPP, confirming the centre of effort with different sail combinations, to test the merits of different sail combinations and investigate interference between the sails. Utilizing three sail plans, full sail, reduced rig which is around 50% of the sail area and storm rig which is 27% of the sail area. The test results showed that sail trimming is very sensitive, meaning that small adjustments to the sails can affect the vessel performance (Deakin, 2002).

Another similar report by William C. Lasher & Logan S. Flaherty used Computational Fluid Dynamics (CFD) and scale model wind tunnel validation to analyse the survivability of a square-rigged sailing vessel. Using the USS Niagara, which is a brig, CFD analysis was performed to investigate heel angle at different wind speeds and sail configurations to determine the performance of the vessel during bad weather. The scale model validation was performed on a model of a rigged topsail at

different angles of attack ranging from 20° to 90°. The results showed that the CFD results were slightly higher across all angles of attack, it also showed that a certain sail configuration would be safe for most expected wind conditions experienced (Lasher & Flaherty, 2014).

With the push to decarbonize, some industry leaders are reviewing the use of wind power to assist in propulsion or in some designs to propel the vessel entirely. With this push, new technologies such as the Flettner rotor, suction wing, wing sail and kites have been developed in the 20th and 21st century. Furthermore, classification societies have been developing guidelines for wind assisted vessels and primary wind vessels as well. With these systems becoming commercially available and examples of wind powered vessels operating in coastal and blue waters, the main barrier for wind powered vessels is a lack of experience of crew and an unwillingness to take on risk (The Royal Institution of Naval Architects , 2021).

Due to these reasons, research into sailing vessels, past and present, will help to better understand and develop procedures and designs that will further develop and support the use of wind power. Furthermore, as this technology develops, better and more efficient methods to harness the wind will become available (The Royal Institution of Naval Architects , 2021).

2 Methods

2.1 Model Development and Construction

The model development began with using the principal particulars to find a scale that would be appropriate for the application. This included finding a scale factor that satisfies the Reynolds scaling while still being small enough to induce an atmospheric boundary layer condition. After a few scale factor changes a final scale factor of 1:130 was chosen. This gave the model principal particulars found in Table 1.

Table 1 Model scale principal particulars

Principal particular	Value	Units
Extreme length	0.301	m
Beam	0.077	m
Depth	0.06	m
Draft (Loaded)	0.039	m
Height (Mainmast)	0.286	m
Density of the fluid	1.194	Kg/m^3
Dynamic viscosity	1.837×10^{-5}	Kg/m/s
Flow speed (wind speed)	15	(m/s)
Model scale Reynolds number	2.2×10^5	N/A

When comparing the full-scale Reynolds number, 1.66×10^7, with the scale model Reynolds numbers, 2.2×10^5 a difference of two orders of magnitude can be seen. To further investigate this difference, measurements were taken on the draft image in Figure 3 with it scaled to full scale along with the diameter of the yards and masts of the model. Reynolds number values were then calculated for the largest diameter full scale mainmast and yards and the 1:165 model scale mainmast and yard (Figure 2). These values can be found in Table 2.

Table 2 Reynolds numbers for masts and yards of the full-scale Sirius and model

Name	Diameter (m)	Reynolds Number
Full-scale mainmast	0.643	6.27×10^5
Full scale main course yard	0.592	5.77×10^5
1:165 model mainmast	0.008	7.80×10^3
1:165 model course yard	0.004	3.90×10^3

With the values from Table 2, and using the graph from Figure 2, it shows that the model scale yards and masts have a drag coefficient of around 1, while the full scale mainmast and yard is approaching the turbulent region and therefore the drag coefficient is much at around 0.8. Although this is a major difference, it should be said that the diameters used to calculate the Reynolds numbers are the largest on the vessel and therefore, it is expected that this is a “worst case scenario” and the remaining masts and yards will have a similar drag coefficient to the scale model (Editors of Encyclopaedia, 2019).

To find the relevant sail area a similar vessel survey of ships from the same era or class (full rigged ships) was undertaken. In all 10 vessels were researched and compared in relation to their displacement and sail area and with the estimated displacement of the *HMS Sirius*, a sail area could be determined (Figure 4).

In addition to the similar vessel survey, the sail area to displacement ratio (Equation 1) was also calculated for the HMS Endeavor due to it being the most similar. With equation 1 (Paris, 2018) and Figure 4, a scale factor could be calculated and then used to increase the *HMS Endeavor* sail plan, which is not only the most similar vessel, it's also the most comprehensive.

$$Sail\ Area\ to\ Displacement\ Ratio = \frac{Sail\ Area\ (m^2)}{Displacement\ (t)^{\frac{2}{3}}} \quad (1)$$

With the main parameters found, the model could be designed and constructed. The base of the model was machined out of steel, while the collars and mounting blocks were machined out of aluminium. These mounting blocks also included a system to allow the masts to rotate allowing the sail angle to change which can be seen in Figure 5. For the masts and sails, stainless steel was chosen for its strength and finally a 3d printed fairing was created to represent the hull. The completed model and the draft image comparison can be seen in Figure 3.

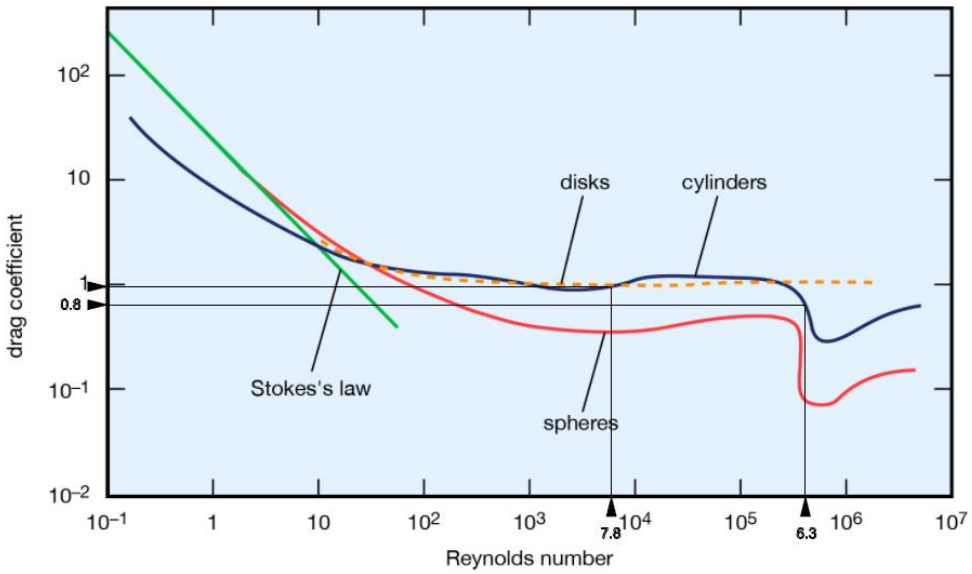

Figure 2 shows that as Reynolds number increases, the drag coefficient changes, however it generally decreases and as it enters the turbulent phase, a clear decrease in drag coefficient can be seen. When comparing the scale model ($3.9x10^3$ & $7.8x10^3$) to the full-scale HMS Sirius ($5.8x10^5$ & $6.3x10^5$) Reynolds numbers, the drag coefficient for the full-scale vessel is approaching the large dip with a lower drag coefficient. However, the dimensions used to calculate these Reynolds numbers are the largest on the vessel and therefore, it is expected that overall, the Reynolds number for the full-scale vessel will be lower and subsequently the drag coefficient will be closer to 1 which is the same as the model. (Editors of Encyclopaedia, 2019).

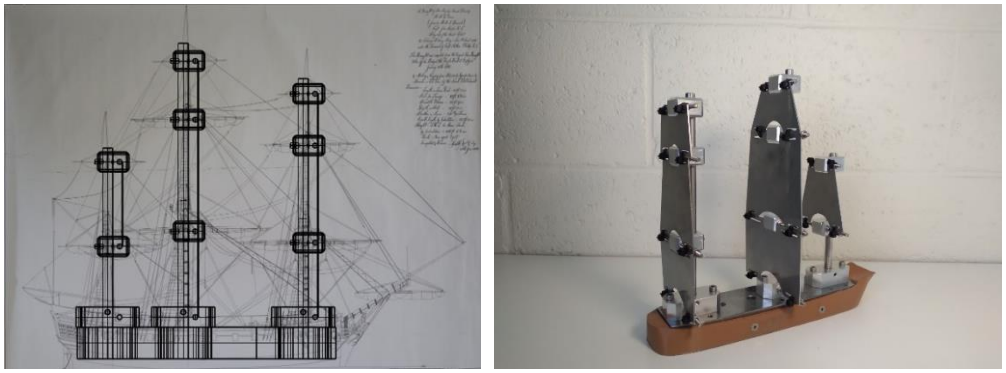

Figure 3 Using the draft image (Left), all major dimensions e.g., mast lengths, positions and yard location on the masts were found. The completed model (Right) includes these dimensions and has the hull fender, which was 3d printed attached to the main structural mounting block. It should also be mentioned that the design includes the ability for the masts to rotate 60 Degrees in 30-degree increments.

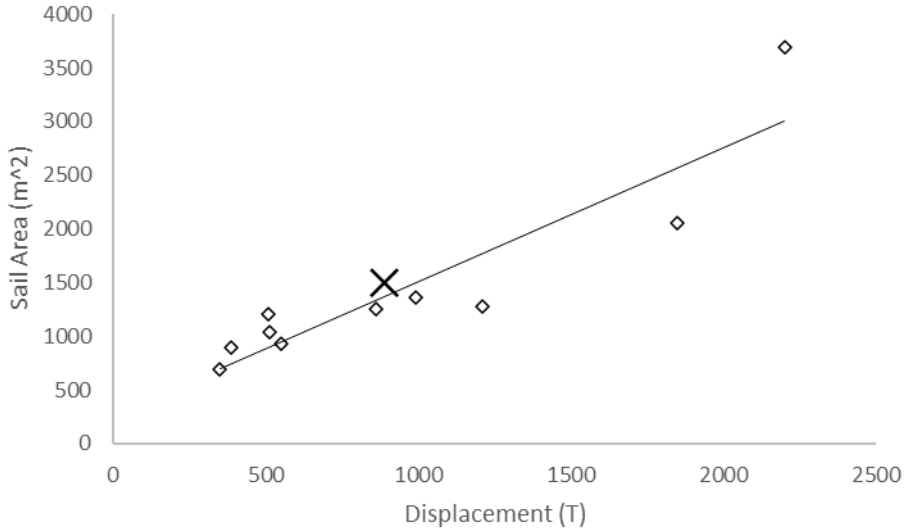

Figure 4 Shows the results of similar vessel survey which includes 10 vessels (*HMS Endeavor, HMS Bounty, HMS Surprise, USS Constitution, Orion Tullan, Vasa, Dom Fernando II e Glória, INS Tarangini, Rainbow Warrior and Sørlandet*). These vessels were chosen due to them being from similar eras and designs. The *HMS Sirius* is denoted by the X.

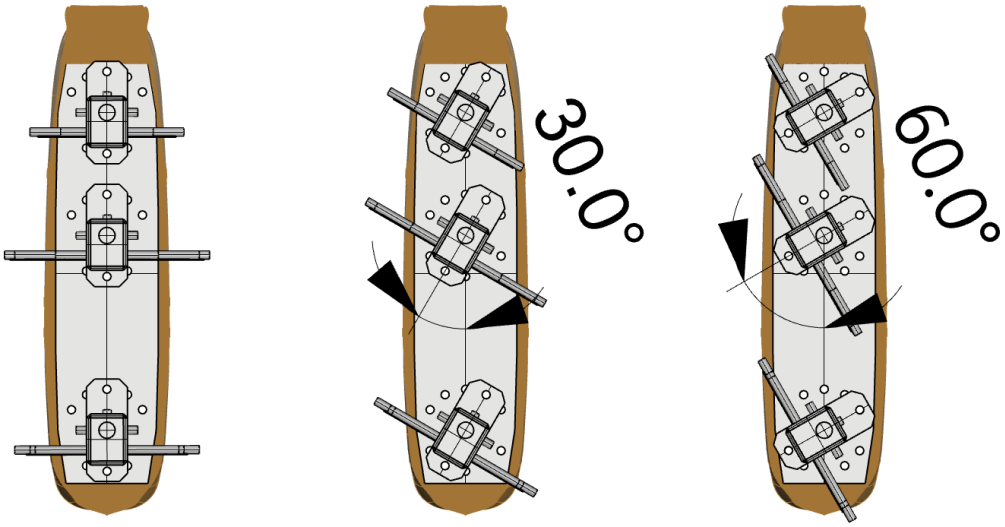

Figure 5 shows the rotation and position of the yards to the main mounting block. During the experiment it is referred to as sail angle e.g., 0° sail (Left), 30° sail (Middle) and 60° sail (Right). This was done to identify the optimal yard and sail angle in relation to the Apparent wind angle.

2.2 Experimental Setup and Procedure

To test the model, the large recirculating wind tunnel facility at the Sandy Bay campus was utilised (Figure 7). During testing it was discovered that the load cell measuring forces in the x axis were not operating correctly. Due to this it was decided to perform the experiment measuring the driving force, and then rotate the load cell 90 degrees so the working load cell would measure the side forces which can be seen in Figure 6. It should also be mentioned that the experiments were carried out with the vessel remaining at a zero-heel angle. This was done to reduce the number of variables within the experiment however it is recommended for further work. The testing consisted of rotating the vessel at 15° apparent wind angle increments and can be seen in Figure 10.

The test matrix consists of 17 five-minute runs with varying wind velocities. This matrix was repeated for each sail rotation and each run needed to be repeated with the load cell rotated 90 degrees. This resulted in a total of 102 test runs and Each 5-minute run had a varying velocity of 5, 10 and 15 m./s (Figure 8 and Figure 9) which was changed at the same time intervals. Using the test matrix, the testing procedure consisted of performing a run at the specified wind angle, then once completed

sometime was allowed for the wind velocity to cease and then the turntable was adjusted to the next wind angle allowing for the process to be repeated. The overall setup and turntable can be seen in Figure 7.

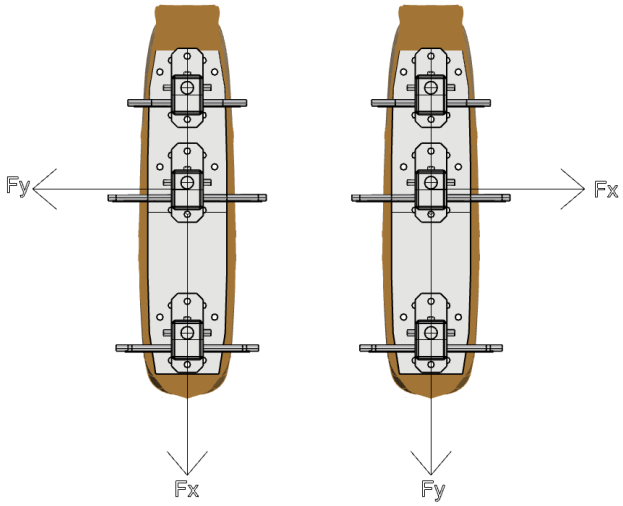

Figure 6 Shows the model with 0° sail angle, compared to the load cell of the wind tunnel. As described, the load cell was not measuring forces in the X axis (Fx) and therefore, it was decided to do the experiment with load cell aligned so the working axis (Fy) would measure the side forces (Left) and then rotated 90 degrees to measure the drive forces (Right).

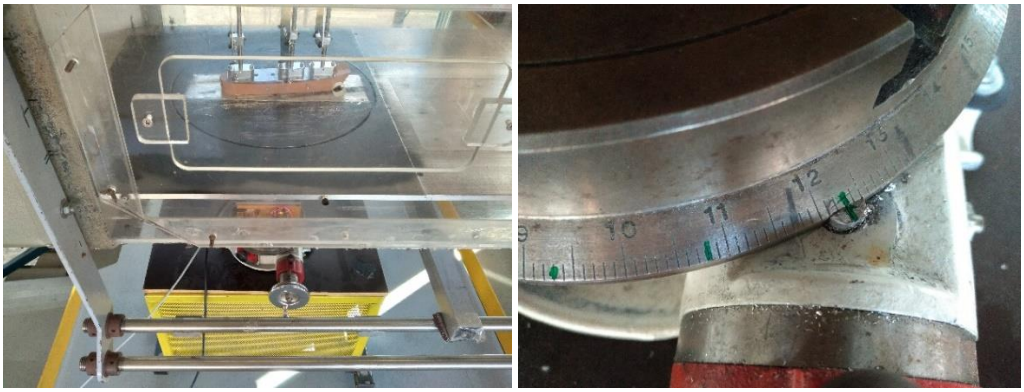

Figure 7 Shows the wind tunnel itself (left) and the turntable (right). For zero-degree AWA drive forces runs, the turntable was set to 123 degrees and 213 degrees for side forces.

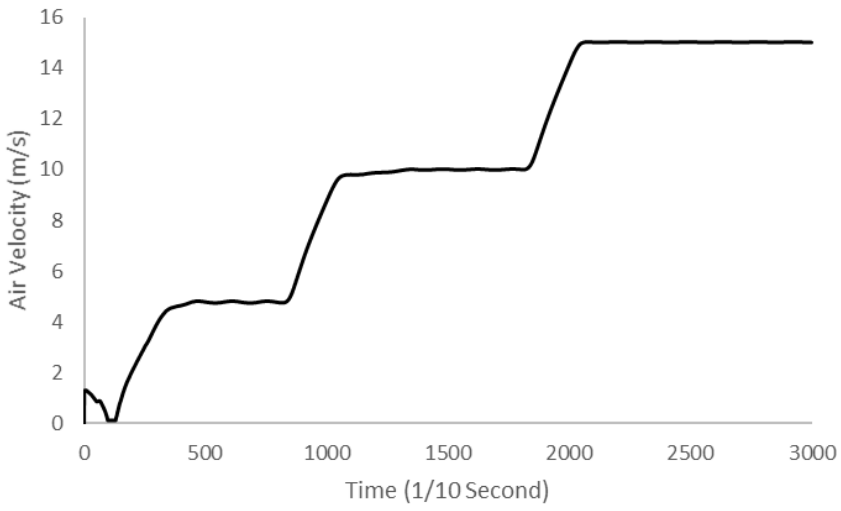

Figure 8 Graph of varying air velocities, the air velocity starts at 5 m/s, then after 80 seconds, the velocity is increased to 10 m/s and held for 100 seconds. Finally, the air velocity was increased to 15 m/s for the final 120 seconds.

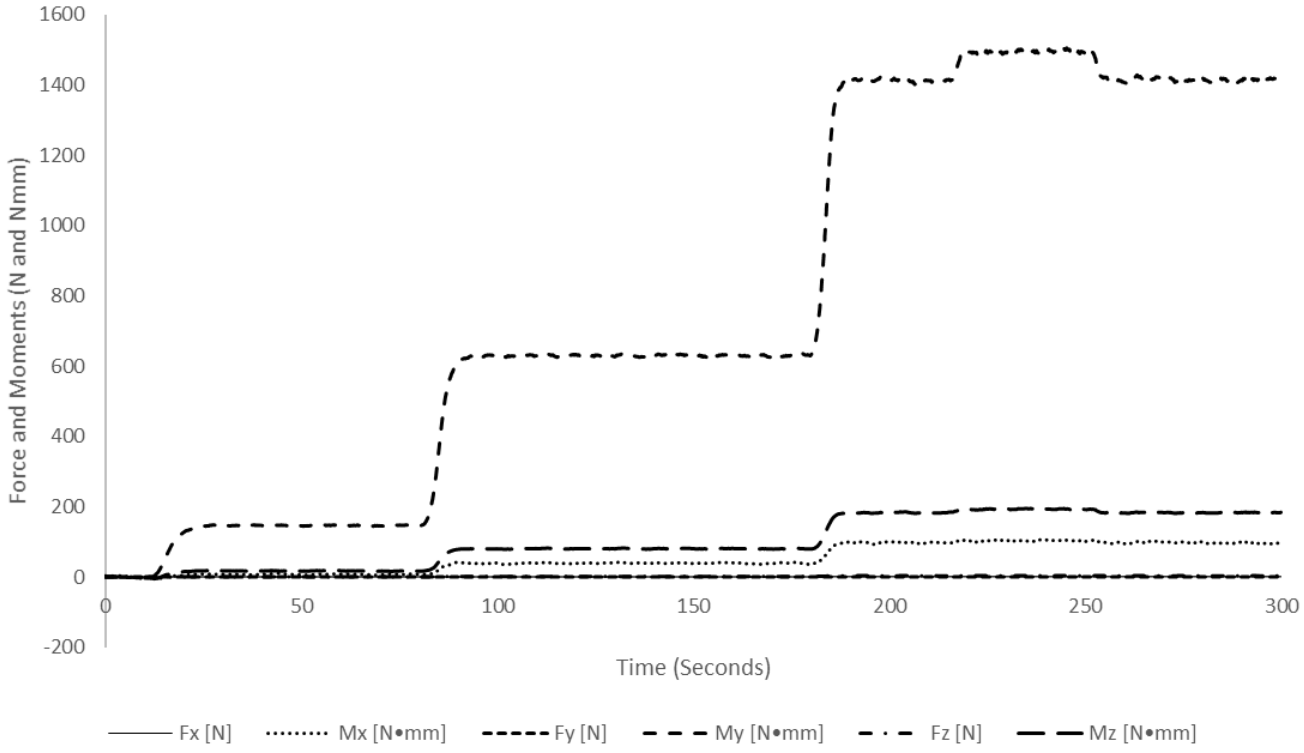

Figure 9 Graph of time compared to forces for 0 AWA 0 Sail (Side force). With all the data collected each run was plotted with time against the forces and moments to ensure all the runs follow a similar trend.

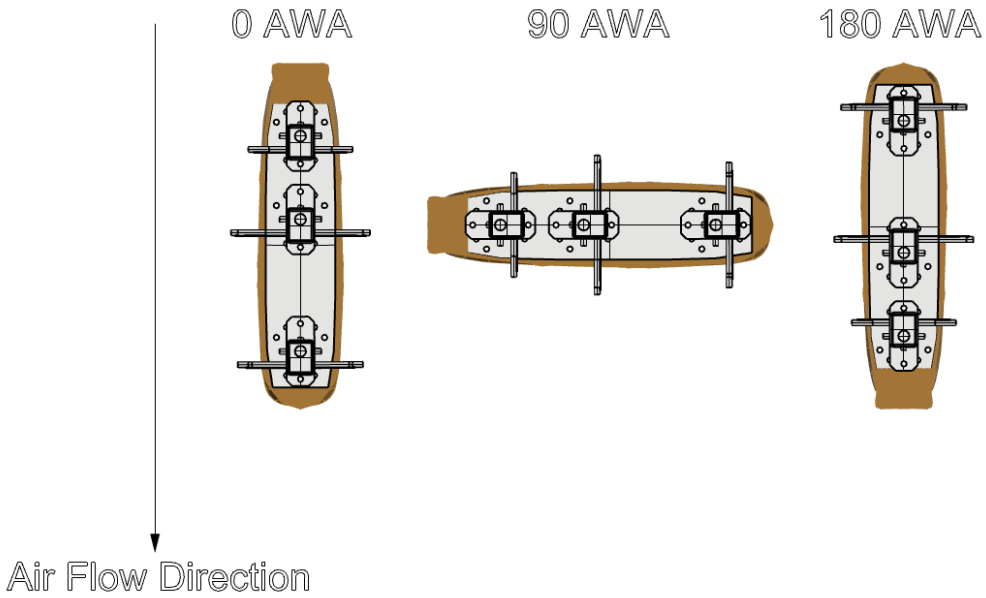

Figure 10 Represents the model in the wind tunnel and shows the model in relation to the air flow direction. As described, the model rotates at 15-degree AWA increments in an anticlockwise direction from 0° AWA (left) through 90° AWA (middle) to 180° AWA (right) with an additional two 15-degree positions at each end of the test matrix (330°, 345°, 195° and 210°). This is known as the Apparent Wind Angle (AWA) Error! Reference source not found.

3 Results and discussion

3.1 Data Processing

With the experiment completed the data was then processed by averaging a portion of the results which would be used to compare with the other runs. It was decided that a ten second window at the end of each velocity which consists of 100 data points per velocity would be adequate to gain a sufficient average. These 10 second windows were from 50 to 60 seconds for 5 m/s, 160 to 170 for 10 m/s and 290 to 300 for 15 m/s. Additionally, the coefficients were also calculated to gain a better value to compare to other experiments.

3.2 Error Analysis

To quantify reliability an uncertainty analysis was undertaken. This involved finding the error in the equipment used during the experiment e.g., Pitot tube, load cells, model sail area and air density. With this information the following equations were used to find the overall uncertainty of the experiment (NASA, 2021).

$$C_{DF}\ or\ C_{SF} = \frac{F}{\frac{1}{2}\,\rho\, V^2\, A} \tag{2}$$

Where:

C_{DF} or C_{SF} = Drive and side force coefficient (non-dimensional value to represent the drag on an object)

F = Force (N)

ρ = Air density (kg/m^3)

V = Air velocity (m/s)

A = Respective surface area, sail area (m^2)

$$\epsilon_{CD} = \sqrt{\left(\epsilon_\rho\left(-2\frac{F_D}{\rho^2\, V^2\, A}\right)\right)^2 + \left(\epsilon_{FD}\left(\frac{1}{\frac{1}{2}\rho^2\, V^2\, A}\right)\right)^2 + \left(\epsilon_V\left(-4\frac{F_D}{\rho\ V^3\, A}\right)\right)^2 + \left(\epsilon_A\left(-2\frac{F_D}{\rho\ V^2\, A^2}\right)\right)^2} \tag{3}$$

Where:

$\epsilon_{DF\ or\ SF}$ = The total error in the experiment

$\epsilon_\rho\ \ \epsilon_{FD}\ \ \epsilon_V\, \epsilon_A$ = The errors related to equation 2

The errors for the relevant experiment are related to the equipment used. For the force, a calibration experiment was done involving the process of slowly adding small weights to the Z axis of the load cell then removing the weight and recording the difference between it and the estimated force (Figure 11) The error for air density and wind velocity is found in the temperature sensor and Setra manometer and finally, the error in the area was found by remeasuring the area of the model at zero AWA (Figure 12). With all the error values calculated (Table 3) equation 2 can be used to find the total error in the experiment.

Table 3 Error values for the experiment

Error Name	Value	Percent Error
Force Error (ϵ_{FD})	0.355 N	8%
Density Error (ϵ_ρ)	1.95x10^{-3} kg/m^3	0.2%
Velocity Error (ϵ_V)	0.294 m/s	2%
Area Error (ϵ_A)	1.4x10^{-4} m^2	2%

With the error calculated for each individual sail condition, these errors were plotted and can be seen in Figure 13 and Figure 14.

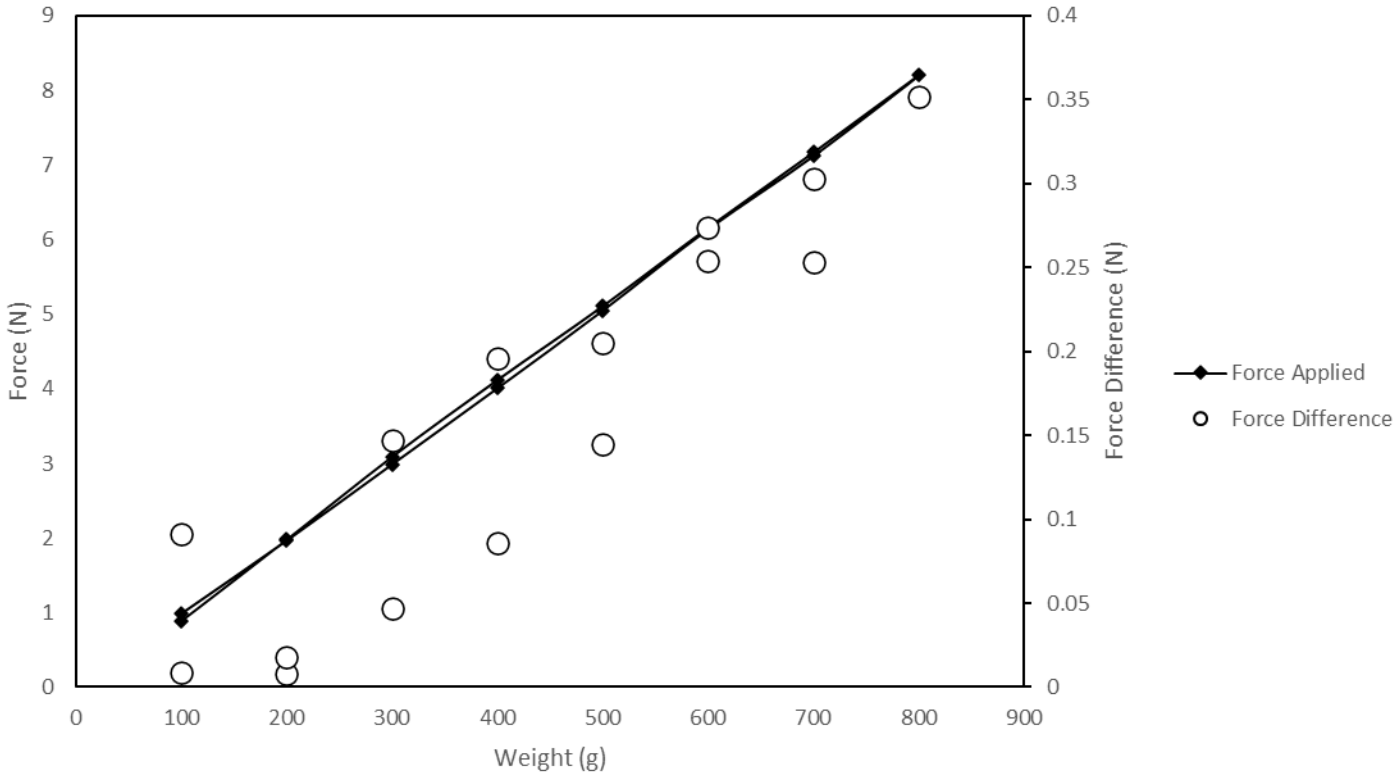

Figure 11 Graph of the applied force from the calibration experiment and the difference between the estimated force and the force from the calibration experiment. It shows that the maximum force difference was 0.355 N which was measured at 800g.

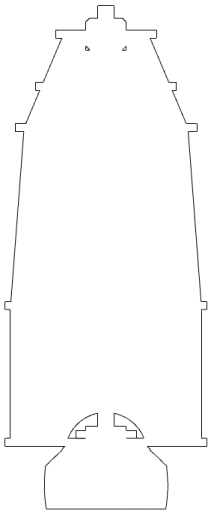

Figure 12 is the silhouette of the proposed area used for the error calculation and to also calculate the coefficient. It is equal to 0.0193 m^2.

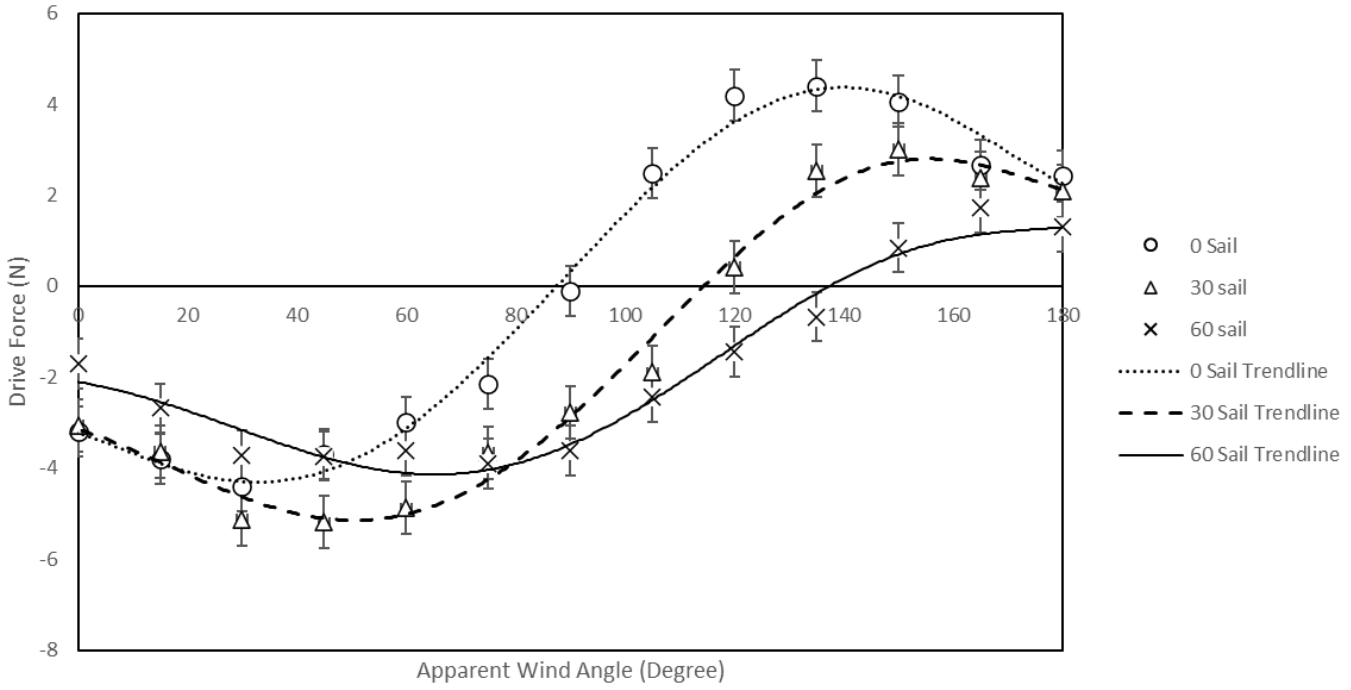

Figure 13 Graph of drive force compared to wind angle and shows drive force against wind angle and when examining the graph, each sail angle stops producing drive force between 80 to 150 degrees. These results can be found in

Table 4.

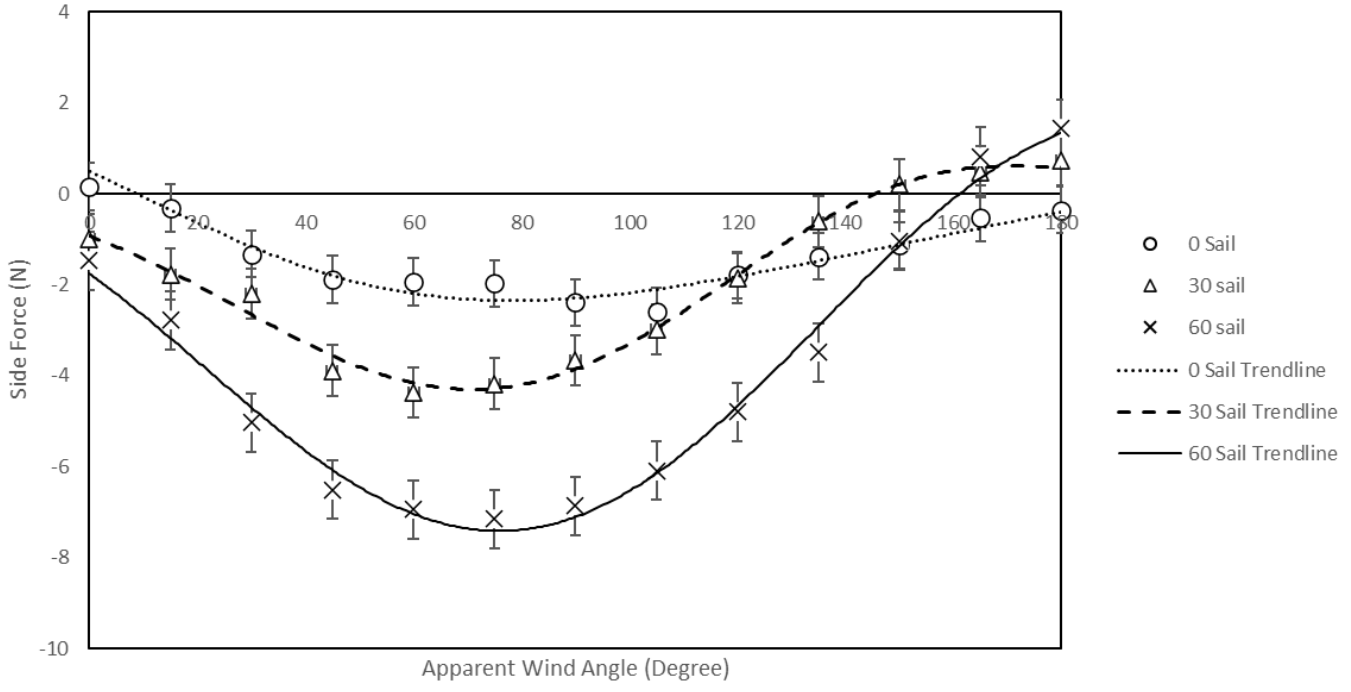

Figure 14 Graph of side force compared to wind angle and shows that the largest side force is generated by the 60-degree sail while the 0 sail produces less side force; has a form of side force present throughout the change in apparent wind angle.

3.3 Results

To compare the results from the experiment the coefficients were calculated for 15m/s wind velocity. These coefficients were then compared between 0°, 30° and 60° sail angle and can be seen below in Figure 15 and Figure 16.

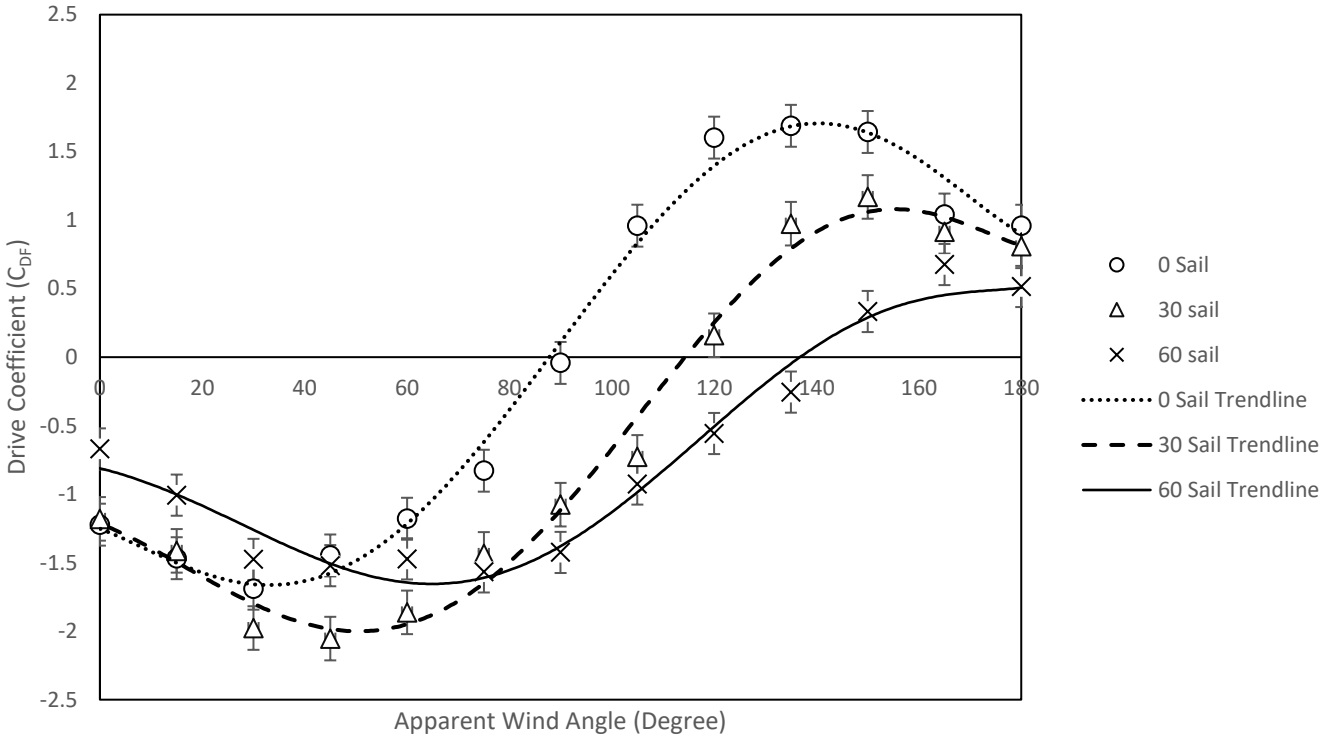

Figure 15 Graph of drive Coefficient compared to wind angle, when examining this graph, it can be said that due to the 60-degree sail having the largest area, it will also produce the largest coefficient. For the 0 and 30 sail set, there is an obvious outlier which occurs at 90 degree and 120 wind angles. This can be explained by the fact that at this angle, the model has little to no sail area contacting the wind flow. This shows that the vessel will completely lose all drive and be completely exposed to side forces.

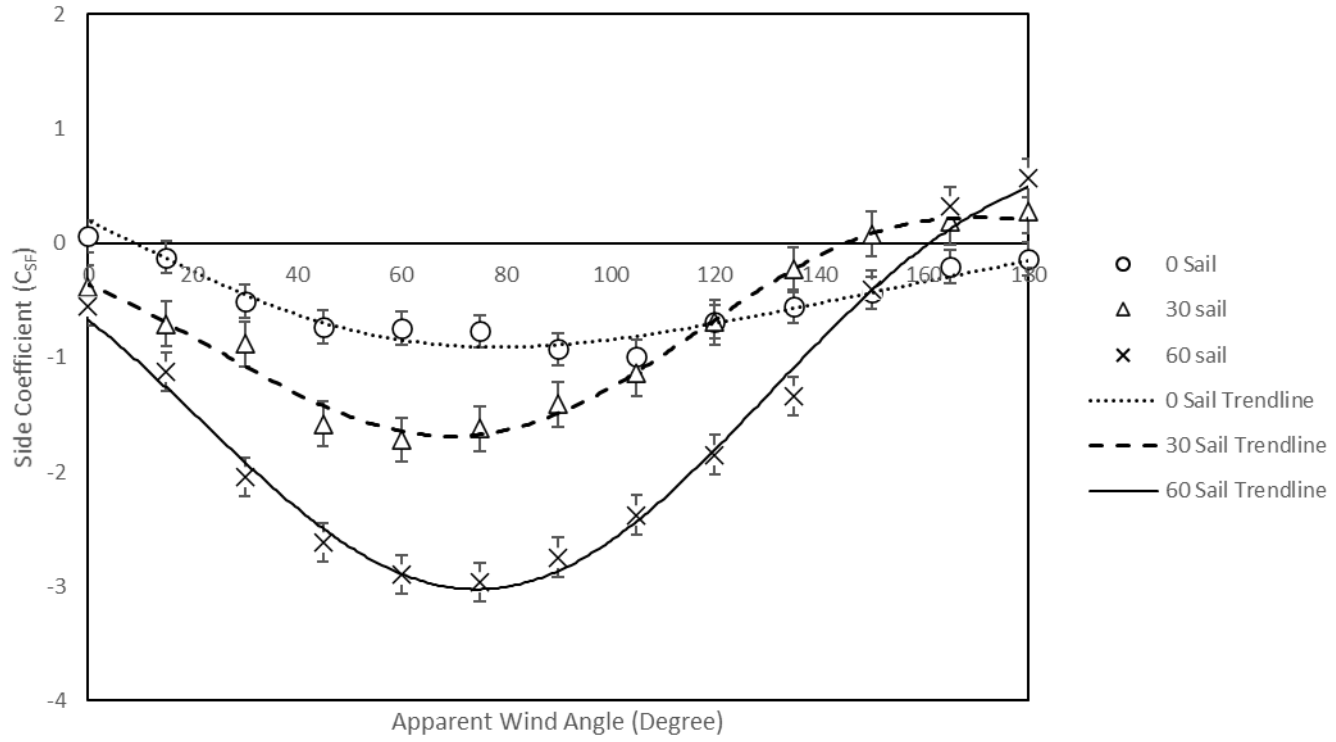

Figure 16 Graph of side coefficient compared to wind angle, when examining the data, it can be said it represents the side force figure (Figure 14).

Table 4 Results for drive force

Sail Angle (Degrees)	Apparent Wind Angle (Degrees)	Drive Force Coefficient
0° Sail	77.5	-0.5
30° Sail	104	-0.5
60° Sail	120	-0.5

The results in the table above (Table 4) shows what apparent wind angle is required to generate a drive coefficient of 0.5 or 1.3 N. This coefficient value was chosen due to the *HM Bark Endeavor* experiments showing a drastic drop in drive force coefficient at around 120 apparent wind angle and can be seen in Figure 17 (Gauntlett, 1994). This gives a standard sailing point that can be used to find the side force coefficients. As shown in Table 4, the 0° sail produces a -0.5 coefficient at 77.5°, the 30° sail is 104° and the 60° sail is 120°. This makes the difference between 0° to 30° sail 26.5° and for 30° to 60° it's 16°.

Table 5 Results for side force

Sail Angle (Degrees)	Apparent Wind Angle (Degrees)	Side Force Coefficient
0° Sail	77.5	-0.88
30° Sail	104	-1.3
60° Sail	120	-1.8

Table 5 shows the resulting side force at the respective apparent wind angle from Table 4. When examining the results, it shows that the difference for side force coefficient is 0.43 from 0° to 30° sail and 0.5 from 30° to 60° sail.

Table 6 Comparing results between drive force and side force

Sail Angle (Degrees)	Apparent Wind Angle (Degrees)	Drive Force Coefficient	Side Force Coefficient
0° Sail	77.5	-0.5	-0.88
30° Sail	104	-0.5	-1.3
60° Sail	120	-0.5	-1.8

Table 6 simply combines the data from the previous tables and allows for comparison. It can be said as the sail angle increases, so does the apparent wind angle and the generated side force. It can also be said that although the 60° sail condition has the highest apparent wind angle, it also results in the highest side force coefficient and past 30° sail, the side coefficient increases at a greater rate.

3.4 Leeway Angle

The leeway angle is the angle difference between the actual heading of the vessel and the direction of motion. If a vessel sails too close to the wind, it will begin to move more sideways than forward. To estimate this angle, results form a study into the sailing performance of the *HM Bark Endeavor* was used (Gauntlett, 1994). It stated that with a wind speed of 15 knots, a leeway angle of 20.3° is expected. When subtracting this angle from the apparent wind angles in

Table 4, new drive and side force coefficients could be found and compared.

Table 7 Leeway angle comparison

Sail Angle (Degrees)	Apparent Wind Angle (Degrees)	Drive Force Coefficient	Side Force Coefficient
0° Sail	57.2	-1.3	-0.8
30° Sail	83.7	-1.35	-1.6
60° Sail	99.7	-1.14	-2.6

Table 7 shows that with the added leeway angle, the reduction in apparent wind angle results in an increase of drive force coefficients and also an increase in side force coefficient. For 0° sail the drive force coefficient has increased to -1.3 while the side force has decreased by -0.08 to -0.8. The 30° sail condition had a small increase in side drive force coefficient to -1.35 while the side force has also increased from -1.3 to -1.6 and finally, the 60° sail area also increased in side force coefficient from to -1.14 combined with an increase in side force coefficient to -2.6.

3.5 Verification

To verify if these results are reasonable, they were compared to the study into the sailing performance of the *HM Bark Endeavor*. This study focused on the creation of a VPP to better understand the sailing characteristics of the vessel. Even though this study produced similar data in the form of drive and side forces, it does not explain the yard position or sail plan for the results (Gauntlett, 1994). The drive force coefficient data from this study was plotted against the results and can be seen in Figure 17. The verification data does not develop the same force coefficients however, it does not follow similar trends apart from when the vessel approaches the higher apparent wind angles.

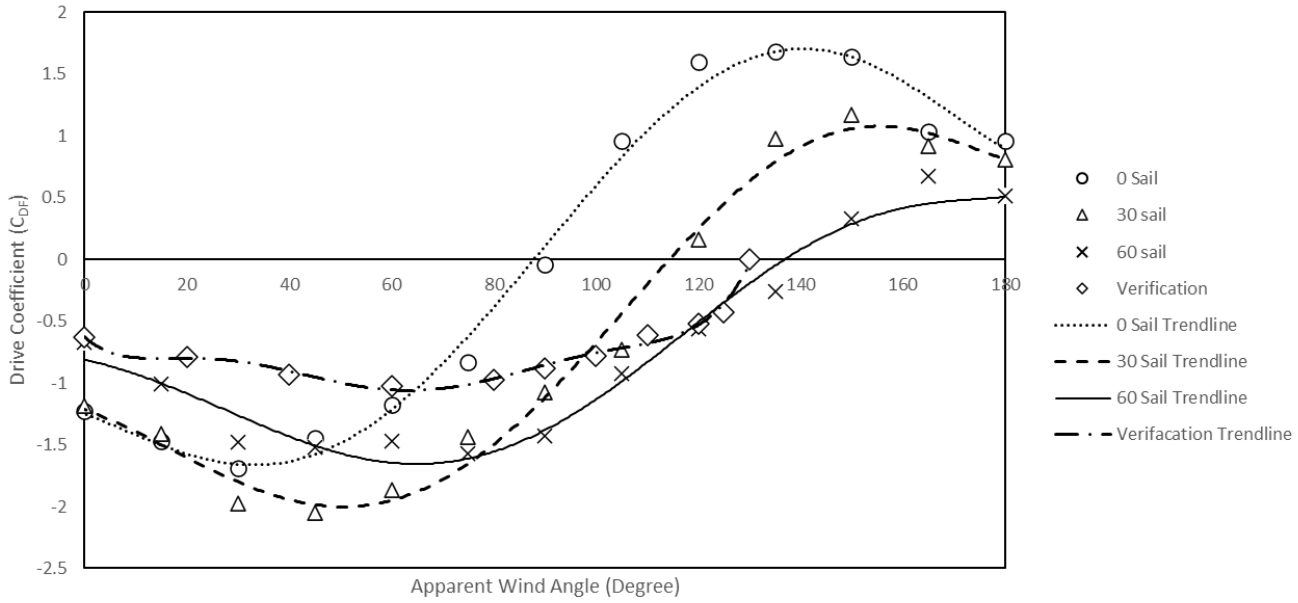

Figure 17 Graph of drive force coefficients including the drive force coefficients for the *HM Bark Endeavor* (Verification). As stated, the verification data does not develop the same drive force coefficients as the experimental data however it does stop developing drive force at a similar point. It also allows for a standard sailing point to be determined which was a coefficient of -0.5. This value was then used in section Error! Reference source not found**..**

4 Conclusions

Overall, the data shows that as the sails rotate, the forces, both drive and side, increase as the vessel itself rotates in the wind tunnel. Using a drive force coefficient of -0.5, it was determined that the resulting apparent wind angles were 77.5° for 0° sail, 104° for 30° sail and 120 for 60° sail. Using these results, the corresponding side force coefficients were then found which were -0.88 for 0° sail, -1.3 for 30° sail and -1.8 for 60° sail. Following this, research into leeway angle found that an estimate of 20.3° leeway angle should be accounted for. This resulted in new apparent wind angles of 57.2° for 0° sail, 83.7° for 30° sail and 99.7° for 60° sail. With these apparent wind angles, the corresponding drive and side force coefficients could be found. For 0° sail the coefficients were -1.3 for drive and -0.8 for side, 30° sail had the coefficients of -1.35 for drive and -1.6 for side and the 60° sail coefficients were -1.14 for drive and -2.6 for side.

With these coefficients calculated it could be concluded that if the drive force is higher than the side force the vessel will certainly generating forward momentum. This condition can be said for the leeway angle adjusted 0° sail which was the only sailing condition to develop more drive force than side force. Although this sailing condition is the only example of drive force being higher than side force, it can also be said that the vessel will still develop forward momentum even if the side force is higher than the drive force. For the leeway angle adjusted 30° sail plan, the difference between the side force and drive force coefficients is 0.25 and therefore it can be said that this condition will also generate forward momentum at and past an apparent wind angle of 83.7°. The 60° sail condition has drastically higher side forces than drive forces throughout the results and for that reason it is expected to be not the ideal sailing condition.

In conclusion, for the vessel to generate forward momentum and make way, an apparent wind angle from 83.7° to 104° with the 30° sail is expected. This is the highest apparent wind angle and after this it is not expected that the vessel will make way.

4.1 Future Work

To further investigate this conclusion, it is recommended that information on the ships resistance and heel angle properties be found. With this an estimation into just how much force is required to propel the vessel could be made. Also, investigation into other sail plans, such as different combinations of degrees could yield a greater apparent wind angle. This will allow for a better understanding into how the *HMS Sirius* handled and performed.

Acknowledgements

I would like to thank Jonathon Binns and Kim Klaka for their continued support and guidance throughout the year. For the physical construction and consulting, I would like to thank Jock Ferguson, Mike Underhill, and Darren Young. For the use of the UTAS wind tunnel, I would like to thank Andrew Bylett and Alan Henderson and finally for technical support during testing, I would like to thank Calverly Gerard.

5 References

Artesania Latina. (2021). *Wooden Model Ship Kit: Swedish Warship Vasa 1/65*. Retrieved from Artesania Latina: https://artesanialatina.net/en/ships-elite/62091-wooden-model-ship-kit-swedish-warship-vasa-1-65-8437021128031.html

Atherton, K. D. (2013, August 19). *The Original Sail Plans for America's Oldest Warship*. Retrieved from Popular Science: https://www.popsci.com/technology/article/2013-08/sail-plans-americas-oldest-warship-document/

Australian National Maritime Museum. (2021). *Ship specifications*. Retrieved from Australian National Maritime Museum: http://www.sea.museum/whats-on/our-fleet/hmb-endeavour/ship-specifications

Deakin, B. (2002). *SAILING SHIP PERFORMANCE - CORRELATION OF MODEL TESTS WITH FULL SCALE*. Southampton: Wolfson unit for marine technology & industrial aerodynamics .

Editors of Encyclopaedia. (2019, October 18). *Reynolds number*. Retrieved from Encyclopædia Britannica: https://www.britannica.com/science/Reynolds-number

Engineers Edge. (2020, November 12). *Viscosity of Air, Dynamic and Kinematic* . Retrieved from Engineers Edge : https://www.engineersedge.com/physics/viscosity_of_air_dynamic_and_kinematic_14483.htm#:~:text=At%2015%20%C2%B0C%2C%20the,the%20kinematic%20viscosity%2015.7%20cSt.

Espin, A. (2010, March 11). *HMS Bounty, Replica* . Retrieved from Eastern Yachts: https://web.archive.org/web/20121102085930/http:/easternyachts.com/bounty/index.htm

Franke, J., Hellsten, A., Schlünzen, H., & Carissimo, B. (2007). *BEST PRACTICE GUIDELINE FOR THE CFD SIMULATION OF FLOWS IN THE URBAN ENVIRONMENT*. Hamburg: University of Hamburg.

Gauntlett, M. J. (1994). *A Scientific Investigation into the Sailing Performance of HM Bark Endeavour*. Perth: Curtin University of Technology.

Greenpeace. (2021). *The Rainbow Warrior*. Retrieved from Greenpeace: https://www.greenpeace.org.au/about/ships/the-rainbow-warrior/

Lasher, W. C., & Flaherty, L. S. (2014). *CFD Analysis of the Survivability of a SquareRigged Sailing Vessel*. Erie: Penn State Erie, The Behrend College, School of Engineering.

Longhurst, A. (2010, May). Sail handling on Endeavour. *Museums quarterly Signals magazine*.

MI News Network. (2021, September 2). *5 Biggest and Magnificent Sailing Ships of All Time*. Retrieved from Marine Insight: https://www.marineinsight.com/types-of-ships/5-biggest-and-magnificent-sailing-ships-of-all-time/

NASA. (2021, MAy 10). *The drag coefficient* . Retrieved from NASA: https://wright.nasa.gov/airplane/drageq.html

Naval Historical society of Australia . (1994, March). *HMS Sirius – Australia's First Flagship*. Retrieved from Naval Historical society of Australia : https://www.navyhistory.org.au/hms-sirius-australias-first-flagship/#:~:text=Her%20extreme%20length%20was%20about,nation%20on%2013th%20May%2C%201787.

Norfolk Island Museum. (2016). *Draught of HMS Sirius*. Retrieved from Norfolk Island Museum: http://norfolkislandmuseum.blogspot.com/2016/12/draught-of-hms-sirius.html

Paris, J. E. (2018, May 31). *Comparing Design Ratios*. Retrieved from Sail Magazine: https://www.sailmagazine.com/boats/comparing-design-ratios

Sail Training International. (2021). *TARANGINI*. Retrieved from Sail on Board: https://sailtraininginternational.org/vessel/tarangini/

Ship Spotting World. (2010, July 7). *HMS Surprise (replica ship)*. Retrieved from Ship Spotting World: http://ship.spottingworld.com/HMS_Surprise_(replica_ship)

Tall Ships America. (2021). *SØRLANDET*. Retrieved from Tall Ships America: https://www.tallshipsamerica.org/vessels/sorlandet/

The Royal Institution of Naval Architects . (2021, January). Wind. *Green Shipping 2021*, pp. 19-24.

War Ships Research. (2016, November 6). *British 3-mast barque (ex-Orion 1945-1949, Tullan 1949-1985) Earl of Pembroke 1985-*. Retrieved from War Ships Research: http://warshipsresearch.blogspot.com/2016/11/british-3-mast-barque-ex-orion-1945.html

War Ships Research. (2018, December 19). *Portuguese frigate Dom Fernando II e Glória 1843-*. Retrieved from War Ships Research: http://warshipsresearch.blogspot.com/2018/12/portuguese-frigate-dom-fernando-ii-e.html

Weather Spark. (2020). *Average Weather on 19 March at Norfolk Island Airport*. Retrieved from Weather Spark: https://weatherspark.com/d/149489/3/19/Average-Weather-on-March-19-at-Norfolk-Island-Airport-Norfolk-Island#Sections-Wind